

FEB 8 1984

C2



# WIND TUNNEL TESTS OF ELEVON GAP HEATING ON THE SPACE SHUTTLE ORBITER (OH-107).

D. W. Stallings  
Calspan Field Services, Inc.

75210

February 1981

Final Report for Period 8 January 1981

Approved for public release; distribution unlimited.

TECHNICAL REPORTS  
FILE COPY

Property of U.S. Air Force  
AEDC LIBRARY  
F40000-81-C-0004

**ARNOLD ENGINEERING DEVELOPMENT CENTER  
ARNOLD AIR FORCE STATION, TENNESSEE  
AIR FORCE SYSTEMS COMMAND  
UNITED STATES AIR FORCE**

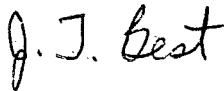
## NOTICES

When U. S. Government drawings, specifications, or other data are used for any purpose other than a definitely related Government procurement operation, the Government thereby incurs no responsibility nor any obligation whatsoever, and the fact that the Government may have formulated, furnished, or in any way supplied the said drawings, specifications, or other data, is not to be regarded by implication or otherwise, or in any manner licensing the holder or any other person or corporation, or conveying any rights or permission to manufacture, use, or sell any patented invention that may in any way be related thereto.

References to named commercial products in this report are not to be considered in any sense as an indorsement of the product by the United States Air Force or the Government.

## APPROVAL STATEMENT

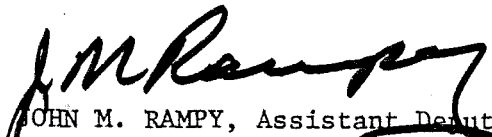
This report has been reviewed and approved.



J. T. BEST  
Aeronautical Systems Division  
Deputy for Operations

Approved for publication:

FOR THE COMMANDER



JOHN M. RAMPY, Assistant Deputy  
Aerospace Flight Dynamics Testing  
Deputy for Operations

UNCLASSIFIED

REPORT DOCUMENTATION PAGE		READ INSTRUCTIONS BEFORE COMPLETING FORM
1. REPORT NUMBER AEDC-TSR-81-V 7	2. GOVT ACCESSION NO.	3. RECIPIENT'S CATALOG NUMBER
4. TITLE (and Subtitle) WIND TUNNEL TESTS OF ELEVON GAP HEATING ON THE SPACE SHUTTLE ORBITER (OH-107)		5. TYPE OF REPORT & PERIOD COVERED Final Report - January 8, 1981
		6. PERFORMING ORG. REPORT NUMBER
7. AUTHOR(s) D. W. Stallings, Calspan Field Services, Inc.		8. CONTRACT OR GRANT NUMBER(s)
9. PERFORMING ORGANIZATION NAME AND ADDRESS Arnold Engineering Development Center/DOS Air Force Systems Command Arnold Air Force Station, TN 37389		10. PROGRAM ELEMENT, PROJECT, TASK AREA & WORK UNIT NUMBERS Program Element 921E01
11. CONTROLLING OFFICE NAME AND ADDRESS NASA/JSC-ES3 Houston, TX 77058		12. REPORT DATE February 1981
		13. NUMBER OF PAGES 24
14. MONITORING AGENCY NAME & ADDRESS (if different from Controlling Office)		15. SECURITY CLASS. (of this report) UNCLASSIFIED
		15a. DECLASSIFICATION/DOWNGRADING SCHEDULE N/A
16. DISTRIBUTION STATEMENT (of this Report) Approved for public release; distribution unlimited.		
17. DISTRIBUTION STATEMENT (of the abstract entered in Block 20, if different from Report)		
18. SUPPLEMENTARY NOTES Available in Defense Technical Information Center (DTIC).		
19. KEY WORDS (Continue on reverse side if necessary and identify by block number) wind tunnel testing space shuttle gap heating		
20. ABSTRACT (Continue on reverse side if necessary and identify by block number) Tests were conducted in the AEDC/VKF Hypersonic Wind Tunnel (B) to obtain heat-transfer rate measurements in the elevon/elevon and elevon/fuselage gap areas of the Space Shuttle Orbiter. Data were obtained at Mach 8 over a Reynolds number range from $0.5 \times 10^6$ to $3.7 \times 10^6$ per foot. Angles of attack of 30, 35, and 40 deg were run for yaw angles of 0 and 1 deg.		

UNCLASSIFIED

## CONTENTS

	<u>Page</u>
NOMENCLATURE . . . . .	2
1.0 INTRODUCTION . . . . .	4
2.0 APPARATUS	
2.1 Test Facility . . . . .	4
2.2 Test Article . . . . .	5
2.3 Test Instrumentation . . . . .	5
3.0 TEST DESCRIPTION	
3.1 Test Conditions . . . . .	6
3.2 Test Procedure . . . . .	6
3.3 Data Reduction . . . . .	6
3.4 Uncertainty of Measurements . . . . .	8
4.0 DATA PACKAGE PRESENTATION . . . . .	8

## APPENDIXES

### I. ILLUSTRATIONS

#### Figure

1. Tunnel B . . . . .	11
2. Photograph of Model . . . . .	12
3. 94-0 Shuttle Orbiter Model . . . . .	13
4. Installation Sketch . . . . .	14
5. Thermocouple Locations . . . . .	15
6. Example Data Plot . . . . .	16

### II. TABLES

#### Table

1. Estimated Uncertainties . . . . .	18
2. Thermocouple Locations and Skin Thicknesses . . . . .	20
3. Test Summary . . . . .	21

### III. REFERENCE HEAT TRANSFER COEFFICIENTS . . . . . 22

### IV. SAMPLE TABULATED DATA

#### Sample

1. Heat Transfer Data . . . . .	24
---------------------------------	----

# NOMENCLATURE

ALPI	Indicated pitch angle, deg
ALPHA	Angle of attack, deg
ALPPB	Prebend angle, deg
B	Model skin thickness, in.
c	Model material specific heat, Btu/lbm-°R
DELTA E	Elevon deflection angle, deg
DTW/DT	Derivative of the model wall temperature with respect to time, °R/sec
H(REF)	Reference heat transfer coefficient (see Appendix III)
H(RTT)	Heat transfer coefficient based on (R)(TT) where R is a predetermined constant, $QDOT/[ (R)(TT) - TW ]$ , Btu/ft <sup>2</sup> -sec-°R
H(TR)	Heat transfer coefficient based on TR, $QDOT/(TR-TW)$ , Btu/ft <sup>2</sup> -sec-°R
H(TT)	Heat transfer coefficient based on TT, $QDOT/(TT-TW)$ , Btu/ft <sup>2</sup> -sec-°R
M	Free-stream Mach number
MODEL	Rockwell model designation
MU	Dynamic viscosity base on free-stream temperature, lbf-sec/ft <sup>2</sup>
P	Free-stream static pressure, psia
PHII	Indicated roll angle, deg
PT	Tunnel stilling chamber pressure, psia
Q	Free-stream dynamic pressure, psia
QDOT	Heat-transfer rate, Btu/ft <sup>2</sup> -sec
RE	Free-stream unit Reynolds number, ft <sup>-1</sup>
RHO	Free-stream density, lbm/ft <sup>3</sup>
RN	Reference nose radius, ft
RUN	Data set identification number
ST(REF)	Stanton number based on reference conditions (see Appendix III)

T	Free-stream static temperature, °R
TC	Thermocouple identification number
TI	Initial wall temperature before injection into the flow, °R
TIME	Elapsed time from lift-off, sec
TR	Assumed recovery temperature, °R
TT	Tunnel stilling chamber temperature, °R
TW	Model surface temperature, °R
V	Free-stream velocity, ft/sec
YAW	Yaw angle, deg
XO	Full-scale model station in axial direction measured from reference point ahead of model, see Fig. 3 and Table 2, in.
YO	Full-scale model station measured from the model centerline in the yaw plane, see Figs. 3 and Table 2, in.
$\rho$	Model material density, lbm/ft <sup>3</sup>

## 1.0 INTRODUCTION

The work reported herein was conducted by the Arnold Engineering Development Center (AEDC), Air Force Systems Command (AFSC), under Program Element 921E01, Control Number 9E01-00-1, at the request of the National Aeronautics and Space Administration, Johnson Space Center (NASA/JSC) for the Rockwell International Corporation. The NASA/JSC project manager was Mrs. D. B. Lee and the Rockwell project engineer was Mr. Paul Lemoine. The results were obtained by Calspan Field Services, Inc./AEDC Division, operating contractor for the Aerospace Flight Dynamics testing effort at the AEDC, AFSC, Arnold Air Force Station, Tennessee. The tests were conducted in the von Karman Gas Dynamics Facility (VKF), under AEDC Project No. C067VB.

As part of the atmospheric flight control system, each wing of the Space Shuttle Orbiter has two elevons on the trailing edge. Since these elevons must move independently, there is a gap between them, and there is also a gap between the inboard elevon and the fuselage. During reentry flight, the pressure on the lower surface of the wing will be much higher than on the upper surface. This will cause significant air flow, with attendant aerodynamic heating, in the gap areas. If the heat-transfer rate is very high, it may be necessary to provide additional insulation in the gap regions to protect the elevon structure. The purpose of this test was to obtain heating-rate data in and around the gaps. This information can then be used to evaluate insulation requirements.

The tests were conducted in Tunnel B at Mach 8 over a Reynolds number range from  $0.5 \times 10^6$  to  $3.7 \times 10^6$  per foot. Model angles of attack of 30, 35, and 40 deg were run at yaw angles of 0 and 1 deg.

All test data, including detailed logs and other information required to use the data, have been transmitted to Rockwell. Inquiries to obtain copies of the test data should be directed to NASA/JSC-ES3, Houston, TX 77058. A microfilm record has been retained in the VKF at AEDC.

## 2.0 APPARATUS

### 2.1 TEST FACILITY

Tunnel B (Fig. 1) is a closed circuit hypersonic wind tunnel with a 50-in.-diam test section. Two axisymmetric contoured nozzles are available to provide Mach numbers of 6 and 8 and the tunnel may be operated continuously over a range of pressure levels from 20 to 300 psia at Mach number 6, and 50 to 900 psia at Mach number 8, with air supplied by the VKF main compressor plant. Stagnation temperatures sufficient to avoid air liquefaction in the test section (up to 1,350°R) are obtained through the use of a natural gas-fired combustion heater. The entire tunnel

(throat, nozzle, test section, and diffuser) is cooled by integral, external water jackets. The tunnel is equipped with a model injection system, which allows removal of the model from the test section while the tunnel remains in operation. A description of the tunnel may be found in the Test Facilities Handbook\*.

## 2.2 TEST ARTICLE

In order to maximize the model scale without blocking the wind tunnel, a partial model, with the right wing cut away, was used. During previous tests data were obtained to define the area which could be removed without influencing the flow field over the remainder of the model. Blockage tests were also carried out to establish the maximum allowable model size. The resulting model was a 0.025-scale version of the Space Shuttle Orbiter, with the Rockwell designation 94-0. It was used originally in a test to determine boundary-layer transition effects on the wing lower surface.

For the present test the 94-0 model was modified to include thin-skin areas on and around the elevons. A photograph of the model is shown in Fig. 2 and a sketch illustrating pertinent details and dimensions is presented in Fig. 3. It was constructed of 17-4 PH stainless steel and the areas where the thermocouples were installed had a nominal skin thickness of 0.020 in. This model did not incorporate the OMS pods, body flap, or vertical tail. Brackets were used to attach the elevons to the trailing edge of the wing. Three sets of these brackets were available to provide elevon deflection angle settings of 0, 2, and 5 deg.

Installation of the model in Tunnel B utilized the components shown in Fig. 4.

## 2.3 TEST INSTRUMENTATION

The instrumentation, recording devices, and calibration methods used to measure the primary tunnel and test data parameters are listed in Table 1a along with the estimated measurement uncertainties. The range and estimated uncertainties for primary parameters that were calculated from the measured parameters are listed in Table 1b.

The model temperatures were measured with Chromel-Constantan<sup>®</sup> thermocouples. The thermocouple locations are shown in Fig. 5 and their coordinates and corresponding skin thicknesses are listed in Table 2.

---

\*Test Facilities Handbook (Eleventh Edition). "von Karman Gas Dynamics Facility Vol. 3." Arnold Engineering Development Center, June 1979.



### 3.0 TEST DESCRIPTION

#### 3.1 TEST CONDITIONS

A summary of the nominal test conditions is given below;

<u>M</u>	<u>PT, psia</u>	<u>TT, °R</u>	<u>RE x 10<sup>-6</sup>, ft<sup>-1</sup></u>
8.0	115	1350	0.5
↓	220	↓	1.0
	445		2.0
	695		3.0
↓	870		3.7

A test summary showing the configurations tested and the variables for each is presented in Table 3.

#### 3.2 TEST PROCEDURE

The model was mounted on a sting support mechanism in the installation tank directly beneath the tunnel test section. The tank is separated from the operating tunnel by a pair of fairing doors and a safety door. The fairing doors cover the opening to the installation tank when closed except for a slot for the pitch sector. The safety door provides a pressure seal between the tunnel and installation tank.

Prior to each test run, the model temperatures were monitored to ensure that they were nominally 80°F. The model was then injected at the desired test attitude as the data acquisition sequence commenced. The model remained on the tunnel centerline for about three seconds and was then retracted into the installation tank. The model was then cooled and repositioned for the next injection.

A 256-channel multiplexing analog-to-digital converter was used in conjunction with a Digital Equipment Corporation® (DEC) PDP-11 computer and a DEC-10 computer to record the temperature data. The converter sampled the output of each thermocouple approximately 17 times per second.

#### 3.3 DATA REDUCTION

##### 3.3.1 Thin-Skin Thermocouple Data

The reduction of thin-skin temperature data to coefficient form normally involves only the calorimeter heat balance for the thin skin as follows:

$$QDOT = \rho Bc DTW/DT \quad (1)$$

$$H(TR) = \frac{QDOT}{TR-TW} = \frac{\rho Bc DTW/DT}{TR-TW} \quad (2)$$

Thermal radiation and heat conduction effects on the thin-skin element are neglected in the above relationship and the skin temperature response is assumed to be due to convective heating only. It can be shown that for constant TR, the following relationship is true:

$$\frac{d}{dt} \left( \ln \left[ \frac{TR-TI}{TR-TW} \right] \right) = \frac{DTW/DT}{TR-TW} \quad (3)$$

Substituting Eq. (3) in Eq. (2) and rearranging terms yields:

$$\frac{H(TR)}{\rho Bc} = \frac{d}{dt} \left( \ln \left[ \frac{TR-TI}{TR-TW} \right] \right) \quad (4)$$

By assuming that the value of  $H(TR)/\rho Bc$  is a constant it can be seen that the derivative (or slope) must also be constant. Hence, the term

$$\ln \left[ \frac{TR-TI}{TR-TW} \right]$$

is linear with time. This linearity assumes the validity of Eq. (2) which applies for convective heating only. The evaluation of conduction effects will be discussed later.

The assumption that  $H(TR)$  and  $c$  are constant are reasonable for this test although small variations do occur in these parameters. The variations of  $H(TR)$  caused by changing wall temperature and by transition movement with wall temperature are trivial for the small wall temperature changes that occur during data reduction. The value of the model material specific heat,  $c$ , was computed by the relation

$$c = 0.0797 + (5.556 \times 10^{-5})TW, \text{ (17-4 PH stainless steel)} \quad (5)$$

The maximum variation of  $c$  over the temperature range of interest was less than 1.5 percent. Thus, the assumption of constant  $c$  used to derive Eq. (4) was reasonable. The value of density used for the 17-4 PH stainless steel skin was  $\rho = 490 \text{ lbm/ft}^3$ , and the skin thickness,  $B$ , for each thermocouple is listed in Table 2.

The right side of Eq. (4) was evaluated using a linear least-squares curve fit of 15 consecutive data points to determine the slope. The start of the curve fit coincided with the model arrival on the tunnel centerline. For each thermocouple the tabulated value of  $H(TR)$  was calculated from the slope and the appropriate values of  $\rho Bc$ ; i.e.,

$$H(TR) = \rho Bc \frac{d}{dt} \left( \ln \left[ \frac{TR-TI}{TR-TW} \right] \right) \quad (6)$$

To investigate conduction effects a second value of  $H(TR)$  was calculated at a time one second later. A comparison of these two values was used to identify those thermocouples that were influenced by significant conduction (or system noise). In general, conduction and/or noise effects were found to be negligible.

Since the value of  $TR$  is not known at each thermocouple location it has become standard procedure to use three assumed values of  $TR$ . The assumed values are  $1.0TT$ ,  $0.9TT$ , and  $0.85TT$ . The use of these assumed values of  $TR$  provides an indication of the sensitivity of the heat-transfer coefficients to the value of  $TR$  assumed. As can be noted in the tabulated data, there are large percentage differences in the values of the heat-transfer coefficients calculated from the three assumed values. Therefore, if the data are to be used for flight predictions, the value selected for  $TR$  is obviously very important and is a function of model location and boundary-layer state.

The heat-transfer coefficient calculated from Eq. (4) was normalized using the Fay-Riddell stagnation point coefficient,  $H(REF)$ , with a reference nose radius,  $RN$ , of 0.025 ft (see Appendix III). This corresponds to a nose radius of 1.0 ft on the full-scale vehicle.

### 3.4 UNCERTAINTY OF MEASUREMENTS

In general, instrumentation calibrations and data uncertainty estimates were made using methods recognized by the National Bureau of Standards (NBS). Measurement uncertainty is a combination of bias and precision errors defined as:

$$U = \pm(B + t_{95}S)$$

where  $B$  is the bias limit,  $S$  is the sample standard deviation and  $t_{95}$  is the 95th percentile point for the two-tailed Student's "t" distribution (95-percent confidence interval), which for sample sizes greater than 30 is taken equal to 2.

Estimates of the measured data uncertainties for this test are given in Table 1a. The data uncertainties for the measurements are determined from in-place calibrations through the data recording system and data reduction program.

Propagation of the bias and precision errors of measured data through the calculated data was made in accordance with the work of Thompson and Abernethy\* and the results are given in Table 1b.

### 4.0 DATA PACKAGE PRESENTATION

A sample data tabulation is presented in Appendix IV. This consists of a listing of the tunnel conditions and model configuration and attitude

---

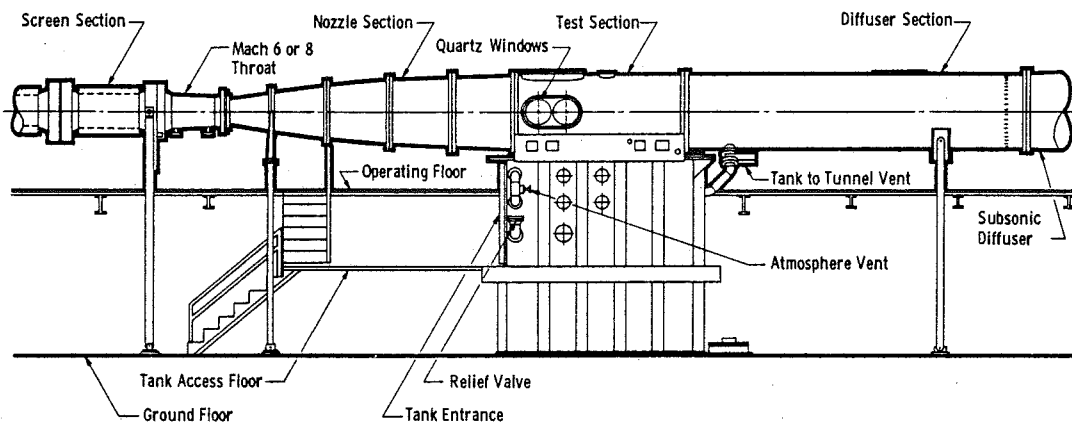
\*Thompson, J. W. and Abernethy, R. B. et al., "Handbook Uncertainty in Gas Turbine Measurements." AEDC-TR-73-5 (AD755356), February 1973.

information for each run, followed by a compilation of the thermocouple data. The thermocouples are listed in order through number 56, and a missing number implies the thermocouple was inoperative for that run. Included for each thermocouple are the temperature at the time of data reduction, the rate-of-change of the temperature (from which the heat-transfer coefficient is calculated), and three values of the heat-transfer coefficient, corresponding to the three assumptions for wall recovery temperature.

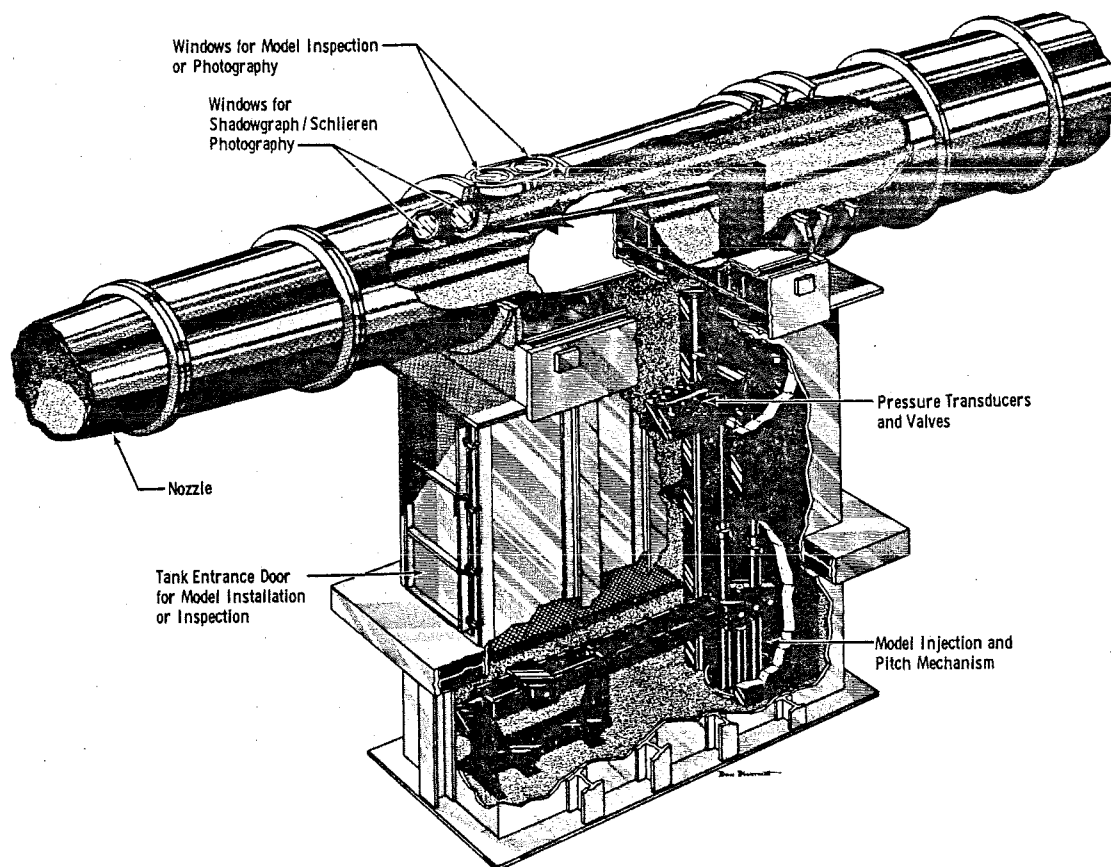
The data were also presented in the form of plots of nondimensional heat-transfer coefficient versus model station. An example of such a plot, with data from the wing lower surface (thermocouples 49 through 56), is shown in Fig. 6. Results are presented for two runs at a Reynolds number of  $3.7 \times 10^6$  per foot, with ALPHA = 30 deg and YAW = 0 deg. The repeatability is excellent. Also included in the figure are data from a previous test (OH-103, a study of heating on the wing lower surface) at the same conditions. Agreement between the two sets of data is quite good.

APPENDIX I

ILLUSTRATIONS



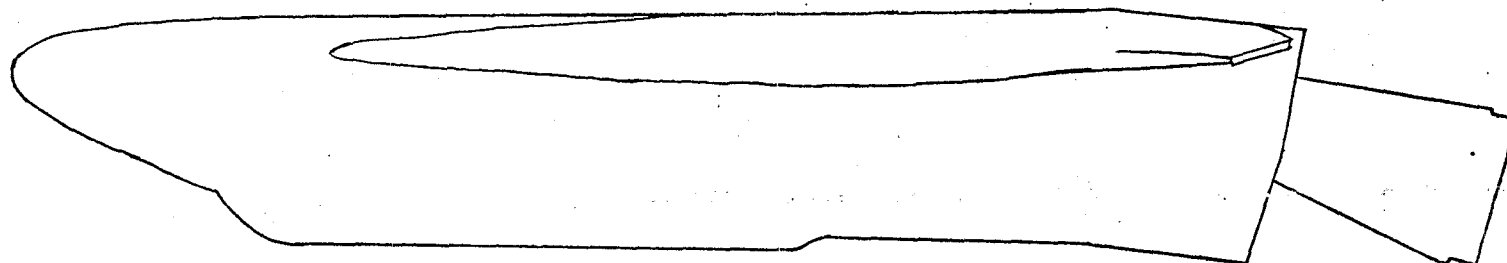
a. Tunnel assembly



b. Tunnel test section  
Fig. 1. Tunnel B



Figure 2. Photograph of Model



Left Side Elevation

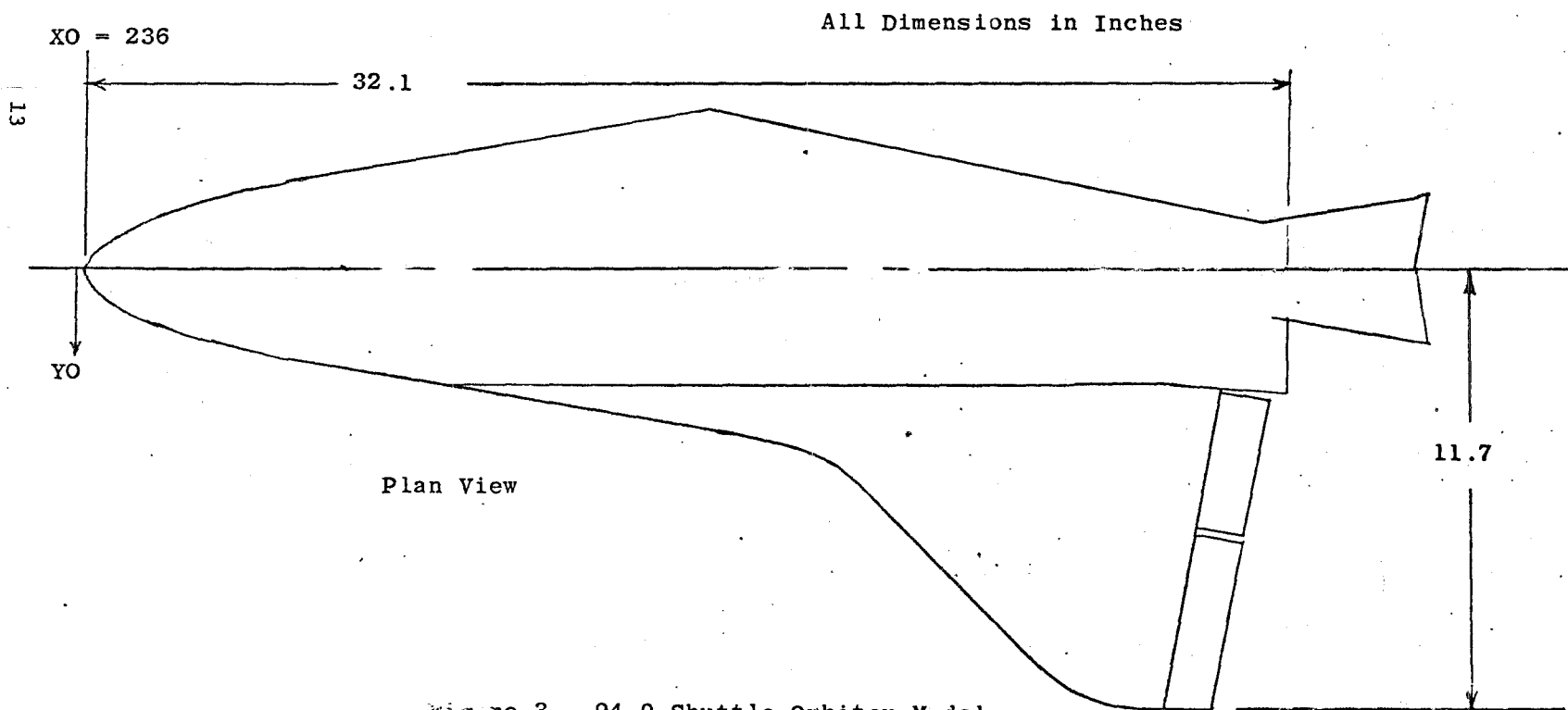


Figure 3. 94-0 Shuttle Orbiter Model



# 50-INCH HYPERSONIC TUNNEL B

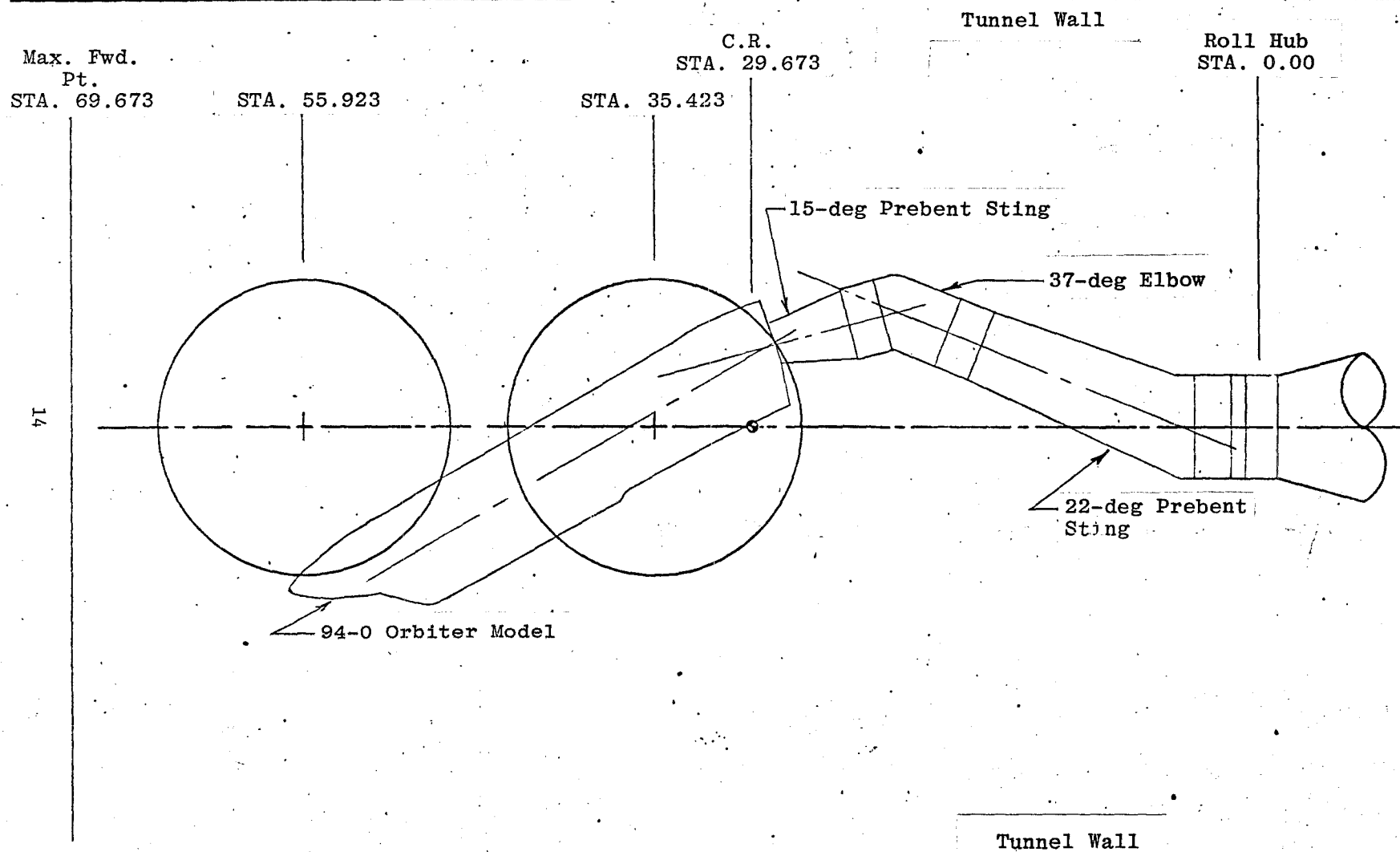


Figure 4. Installation Sketch

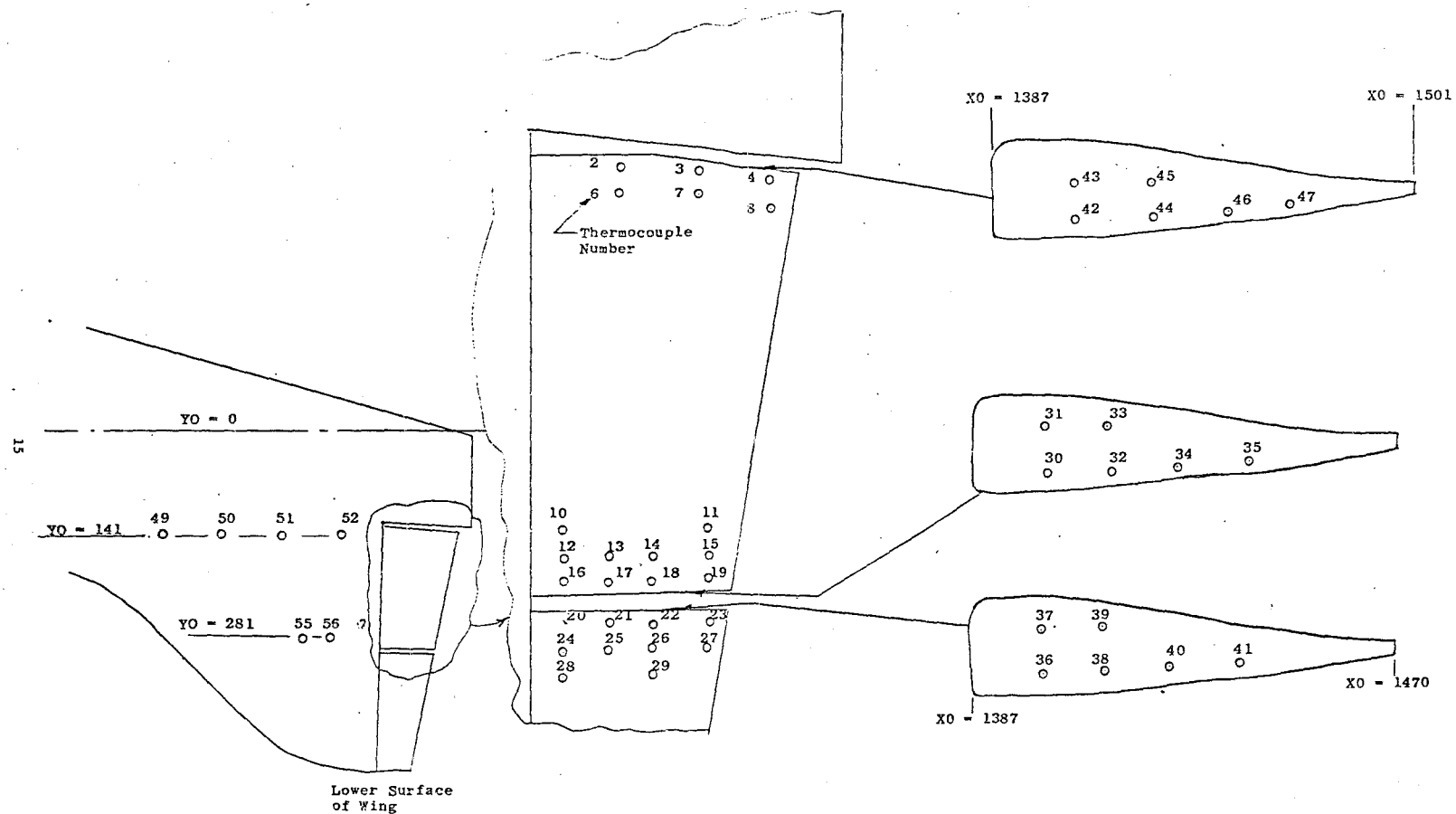


Figure 5. Thermocouple Locations

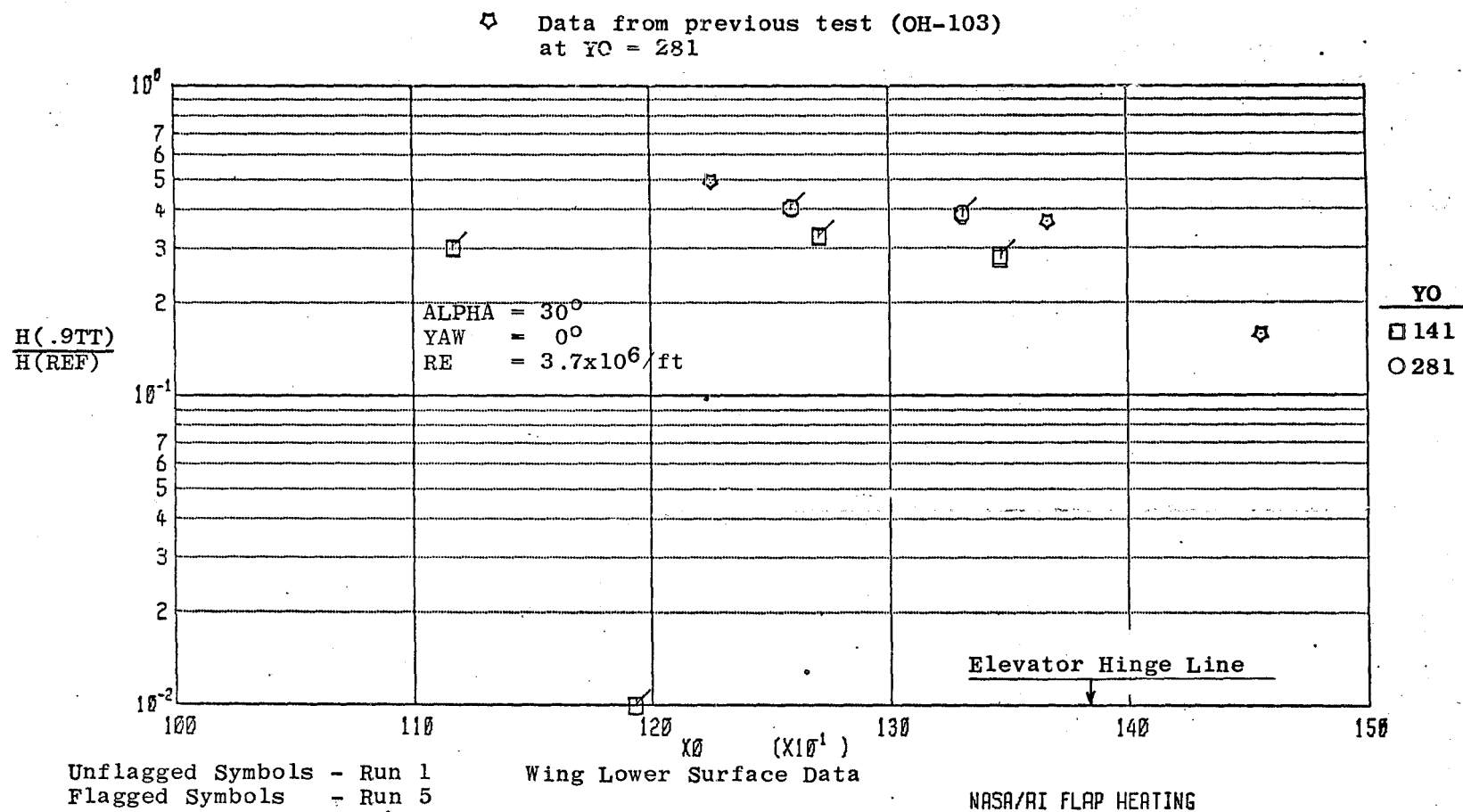


Figure 6. Example Data Plot

APPENDIX II

TABLES

TABLE 1. ESTIMATED UNCERTAINTIES

a. Basic Measurements  
Tunnel B

Parameter Designation	STEADY-STATE ESTIMATED MEASUREMENT*							Range	Type of Measuring Device	Type of Recording Device	Method of System Calibration
	Precision Index (S)			Bias (B)		Uncertainty $\pm(B + t_{95}S)$					
	Percent of Reading	Unit of Measurement	Degree of Freedom	Percent of Reading	Unit of Measurement	Percent of Reading	Unit of Measurement				
ALPI,deg	0.025		>30			$\pm 0.05$		$\pm 11$	Potentiometer	Analog-to-digital converter into data acquisition system	Heidenhain rotary encoder RoD700 Resolution: 0.000 Overall accuracy: 0.001 <sup>o</sup>
PHII,deg	0.15		>30			$\pm 0.3$		$\pm 90$			
PT,psia	0.02		>30		0.26		$\pm 0.3$	$0 < P \leq 104$	Bell & Howell variable capacitance pressure transducer	Analog to Digital Converter into Data Acquisition System	In-place application of multiple pressure levels measured with a pressure measuring device calibrated in the standards laboratory
	0.02		>30	0.25		$\pm (0.25\% + .08 \text{ psi})$	$\pm 0.80$	$104 < P < 200$			
	0.11		>30		0.58		$\pm 0.80$	$200 < P \leq 323$			
	0.11		>30	0.25		$\pm (0.25\% + 0.22 \text{ psi})$		$232 < P \leq 1000$			
TIME,sec	$5 \times 10^{-4}$		>30	[(Runtime in sec) $(5 \times 10^{-6})$ ]		$\pm [(\text{Runtime in sec}) (5 \times 10^{-6}) + 10^{-3}] \text{ sec}$		milli-seconds to 365 days	System Donner time code reader	Digital Data Acquisition System	Instrument lab calibration against NBS
TT, <sup>o</sup> F	1		>30	0.375		$\pm (0.375\% + 2^{\circ} \text{F})$		790-890	Chromel <sup>R</sup> -Alumel <sup>R</sup> Thermocouple	Digital Thermometer into Digital Data Acquisition System	Thermocouple verification of NBS conformity/voltage substitution calibration
TW, <sup>o</sup> F	1		>30	2		$\pm 4$		50-200	CR-CN Thermocouple	Low Level Multiplexer into Analog to Digital Converter into Data Acquisition System	

\*Thompson, J. W. and Abernethy, R. B. et al. "Handbook Uncertainty in Gas Turbine Measurements." AEDC-TR-73-5 (AD 755356), February 1973.

TABLE 1. Concluded  
b. Calculated Parameters

Parameter Designation	STEADY-STATE ESTIMATED MEASUREMENT*							Range
	Precision Index (S)			Bias (B)		Uncertainty $\pm(B + t_{95}S)$		
	Percent of Reading	Unit of Measurement	Degree of Freedom	Percent of Reading	Unit of Measurement	Percent of Reading	Unit of Measurement	
M		$\pm 0.020$ $\pm 0.010$	>30		0+ 0+		$\pm 0.04$ $\pm 0.02$	7.83 8.0
RE, ft <sup>-1</sup>	$\pm 0.70$ $\pm 0.36$		>30	$\pm 0.56$ $\pm 0.45$		$\pm 1.96$ $\pm 1.17$		$0.5 \times 10^6 \text{ft}^{-1}$ $3.7 \times 10^6 \text{ft}^{-1}$
H(TT), H(.9TT), H(.85TT), BTU/ft <sup>2</sup> - sec <sup>-0</sup> R	$\pm 1.0$ $\pm 4.0$		>30 >30	$\pm 6.0$ $\pm 6.0$		$\pm 8.0$ $\pm 14.0$		$> 1 \times 10^{-3}$ $1 \times 10^{-4} \rightarrow$ $1 \times 10^{-3}$
(Thin-skin thermo- couple technique	$\pm 7.0$		>30	$\pm 6.0$		$\pm 20.0$		$< 1 \times 10^{-4}$

\*Abernethy, R. B. et al. and Thompson, J. W. "Handbook Uncertainty in Gas Turbine Measurements."  
AEDC-TR-73-5 (AD 755356), February 1973.  
Assumed to be zero

TABLE 2

## Thermocouple Locations and Skin Thicknesses

Thermocouple Number	Model Stations, in.		Skin Thickness, in.
	XO	YO	
2	1426	134	0.0200
3	1458	139	0.0205
4	1494	144	0.0202
6	1426	144	0.0203
7	1458	149	0.0193
8	1494	154	0.0203
10	1402	282	0.0208
11	1460	282	0.0201
12	1402	292	0.0197
13	1420	↓	0.0213
14	1440	↓	0.0204
15	1460	292	0.0191
16	1402	302	0.0182
17	1420	↓	0.0217
18	1440	↓	0.0208
19	1460	302	0.0197
21	1420	320	0.0220
22	1440	↓	0.0204
23	1460	320	0.0198
24	1402	330	0.0194
25	1420	↓	0.0196
26	1440	↓	0.0190
27	1460	330	0.0210
28	1402	340	0.0192
29	1438	340	0.0190
30	1402	307	0.0201
31	1402	↓	0.0201
32	1420	↓	0.0201
33	1420	↓	0.0201
34	1440	↓	0.0201
35	1452	307	0.0201
36	1402	316	0.0201
37	1402	↓	0.0202
38	1420	↓	0.0202
39	1420	↓	0.0202
40	1440	↓	0.0202
41	1452	316	0.0202
44	1428	128	0.0205
45	1428	134	0.0205
46	1448	130	0.0204
47	1468	136	0.0205
49	1117	141	0.0250
50	1193	↓	0.0290
51	1271	↓	0.0270
52	1347	141	0.0320
54	1259	281	0.0290
55	1295	↓	0.0260
56	1331	281	0.0290

\* Referenced to full scale vehicle

TABLE 3

## Test Summary

ALPHA, deg	YAW, deg	DELTA E, deg	REx10 <sup>-6</sup> , ft <sup>-1</sup>				
			0.5	1.0	2.0	3.0	3.7
30	0	0			51	47	43
30	1				52	48	44
35	0				53	49	45
35	1				54	50	46
40	0		59	57	55		
40	1		60	58	56		
30	0	2			33	29	25
30	1				34	30	26
35	0				35	31	27
35	1				36	32	28
40	0		41	39	37		
40	1		42	40	38		
30	0	5			14, 20	10	1, 5
30	1				15	11	2, 6
35	0				16	12	3, 7, 8
35	1				17	13	4, 9
40	0		23	21	18		
40	1		24	22	19		

RUN NUMBERS →



# APPENDIX III

## REFERENCE HEAT-TRANSFER COEFFICIENTS

In presenting heat-transfer coefficient results it is convenient to use reference coefficients to normalize the data. Equilibrium stagnation point values derived from the work of Fay and Riddell\* were used to normalize the data obtained in this test. These reference coefficients are given by:

$$H(\text{REF}) = \frac{8.17173(\text{PT2})^{1/2}(\text{MUTT})^{0.4} \left[1 - \frac{P}{\text{PT2}}\right]^{0.25} [0.2235 + (1.35 \times 10^{-5})(\text{TT}+560)]}{(\text{RNR})^{1/2}(\text{TT})^{0.15}}$$

and

$$\text{ST}(\text{REF}) = \frac{H(\text{REF})}{(\text{RHO})(\text{V}) [0.2235 + (1.35 \times 10^{-5})(\text{TT} + 560)]}$$

where

PT2	Stagnation pressure downstream of a normal shock wave, psia
MUTT	Air viscosity based on TT, lb <sub>f</sub> -sec/ft <sup>2</sup>
P	Free-stream pressure, psia
TT	Tunnel stilling chamber temperature, °R
RNR	Reference nose radius, ft (RNR = 0.025 ft for this test)
RHO	Free-stream density, lbm/ft <sup>3</sup>
V	Free-stream velocity, ft/sec

---

\*Fay, J. A. and Riddell, F. R. "Theory of Stagnation Point Heat Transfer in Dissociated Air," Journal of the Aeronautical Sciences, Vol. 25, No. 2, February 1958.

APPENDIX IV

SAMPLE TABULATED DATA

ARVIN/CALSON FIELD SERVICES, INC.  
AEDC DIVISION  
VON KARMAN GAS DYNAMICS FACILITY  
ARNOLD AIR FORCE STATION, TENNESSEE  
NASA/RI FLAP HEATING  
PAGE 1

DATE COMPUTED 19-JAN-81  
TIME COMPUTED 11:24:21  
DATE RECORDED 8-JAN-81  
TIME RECORDED 0:40:46  
PROJECT NUMBER V43B-17

RUN	MODEL	M	PT,PSIA	TT,DEGR	ALPPB	ALPI	PHII	ALPHA	YAW	DELTA E
1	94-0	7.97	829.4	1364.7	29.83	-0.26	-0.02	30.09	0.00	5

T	P	Q	V	RHO	MU	RE	H(REF)	ST(REF)
DEGR	PSIA	PSIA	FT/SEC	LB/FT3	LB-SEC/FT2	FT-1	(RM= 0.0250FT)	(RM= 0.0250FT)
99.51	0.087	3.864	3899.	2.355E-03	8.007E-08	3.564E+06	4.090E-02	1.785E-02

TC NO	TW DEG R	DTW/DT DEG S	QDOT BTU/FT2-S	H(TT) BTU/FT2-S-DEG R	H(TT) /H(REF)	H(.9TT) BTU/FT2-S-DEG R	H(.9TT) /H(REF)	H(.85TT) BTU-FT2-S-DEG R	H(.85TT) /H(REF)	B IN.	XO IN.	YO IN.
3	603.4	53.286	5.050	6.634E-03	0.1622	8.084E-03	0.1977	9.075E-03	0.2219	0.0205	1458.	139.
4	608.9	52.633	4.929	6.522E-03	0.1595	7.959E-03	0.1946	8.945E-03	0.2187	0.0202	1494.	144.
6	624.1	61.819	5.861	7.914E-03	0.1935	9.702E-03	0.2372	1.094E-02	0.2674	0.0203	1426.	144.
7	606.6	54.390	4.861	6.413E-03	0.1568	7.821E-03	0.1912	8.785E-03	0.2148	0.0193	1458.	149.
8	595.8	47.181	4.412	5.737E-03	0.1403	6.975E-03	0.1706	7.819E-03	0.1912	0.0203	1494.	154.
10	633.0	66.832	6.520	8.912E-03	0.2179	1.096E-02	0.2679	1.237E-02	0.3026	0.0208	1402.	282.
11	622.3	62.354	5.848	7.878E-03	0.1926	9.653E-03	0.2360	1.088E-02	0.2660	0.0201	1460.	282.
12	645.3	71.763	6.670	9.272E-03	0.2267	1.144E-02	0.2798	1.296E-02	0.3169	0.0197	1402.	292.
13	633.1	68.345	6.828	9.333E-03	0.2282	1.147E-02	0.2805	1.296E-02	0.3169	0.0213	1420.	292.
14	614.7	53.285	5.054	6.739E-03	0.1648	8.238E-03	0.2014	9.269E-03	0.2266	0.0204	1440.	292.
15	630.3	71.808	6.425	8.749E-03	0.2139	1.075E-02	0.2628	1.213E-02	0.2966	0.0191	1460.	292.
16	652.3	70.197	6.048	8.490E-03	0.2076	1.050E-02	0.2568	1.191E-02	0.2913	0.0182	1402.	302.
17	637.3	74.804	7.630	1.049E-02	0.2565	1.291E-02	0.3157	1.460E-02	0.3569	0.0217	1420.	302.
19	632.8	73.570	6.797	9.288E-03	0.2271	1.142E-02	0.2791	1.289E-02	0.3153	0.0197	1460.	302.
21	661.9	86.304	9.030	1.285E-02	0.3142	1.595E-02	0.3899	1.813E-02	0.4433	0.0220	1420.	320.
22	652.9	73.527	7.103	9.979E-03	0.2440	1.235E-02	0.3019	1.401E-02	0.3425	0.0204	1440.	320.
23	670.9	93.887	8.879	1.280E-02	0.3129	1.593E-02	0.3895	1.815E-02	0.4439	0.0198	1460.	320.
24	650.4	71.024	6.517	9.125E-03	0.2231	1.128E-02	0.2750	1.279E-02	0.3128	0.0194	1402.	330.
25	628.9	67.612	5.204	8.432E-03	0.2062	1.035E-02	0.2531	1.168E-02	0.2856	0.0196	1420.	330.
26	610.9	55.489	4.892	6.490E-03	0.1587	7.925E-03	0.1938	8.910E-03	0.2179	0.0190	1440.	330.
27	625.4	70.843	6.952	9.404E-03	0.2299	1.153E-02	0.2820	1.300E-02	0.3180	0.0210	1460.	330.
28	657.1	73.957	6.738	9.523E-03	0.2328	1.180E-02	0.2885	1.340E-02	0.3276	0.0192	1402.	340.
29	612.4	52.269	4.612	6.131E-03	0.1499	7.489E-03	0.1831	8.422E-03	0.2059	0.0190	1438.	340.
30	532.1	18.001	1.614	1.939E-03	0.0474	2.319E-03	0.0567	2.571E-03	0.0629	0.0201	1402.	307.
31	516.9	3.153	0.281	3.309E-04	0.0081	3.944E-04	0.0096	4.363E-04	0.0107	0.0201	1402.	307.
32	535.2	20.701	1.859	2.241E-03	0.0548	2.683E-03	0.0656	2.976E-03	0.0728	0.0201	1420.	307.
33	538.4	15.181	1.366	1.653E-03	0.0404	1.980E-03	0.0484	2.197E-03	0.0537	0.0201	1420.	307.
35	553.5	25.426	2.305	2.842E-03	0.0695	3.416E-03	0.0835	3.801E-03	0.0929	0.0201	1452.	307.
36	607.9	57.225	5.330	7.043E-03	0.1722	8.593E-03	0.2101	9.655E-03	0.2361	0.0201	1402.	316.
37	528.1	11.333	1.019	1.218E-03	0.0298	1.456E-03	0.0356	1.613E-03	0.0394	0.0202	1402.	316.
38	622.2	73.850	6.961	9.375E-03	0.2292	1.149E-02	0.2809	1.294E-02	0.3165	0.0202	1420.	316.
39	540.7	25.351	2.295	2.785E-03	0.0681	3.338E-03	0.0816	3.705E-03	0.0906	0.0202	1420.	316.
40	622.0	77.616	7.315	9.850E-03	0.2409	1.207E-02	0.2951	1.360E-02	0.3325	0.0202	1440.	316.
41	666.1	90.744	8.735	1.250E-02	0.3057	1.554E-02	0.3800	1.769E-02	0.4325	0.0202	1452.	316.
44	545.8	19.079	1.757	2.146E-03	0.0525	2.575E-03	0.0630	2.861E-03	0.0700	0.0205	1428.	128.
45	523.9	7.840	0.714	8.494E-04	0.0208	1.014E-03	0.0248	1.123E-03	0.0275	0.0205	1428.	134.
46	535.8	10.618	0.968	1.168E-03	0.0286	1.398E-03	0.0342	1.551E-03	0.0379	0.0204	1448.	130.
47	538.9	13.824	1.269	1.537E-03	0.0376	1.841E-03	0.0450	2.043E-03	0.0500	0.0205	1468.	136.